International Journal of Applied Mathematics
Volume 38 No. 10s, 2025
ISSN: 1311-1728 (printed version); ISSN: 1314-8060 (on-line version)

HIGH ISOLATION FOUR ANTENNA UWB MIMO USING PROTRUDENT SHAPED ELEMENTS FOR WLAN BAND REJECTION CAPABILITIES

Sujeet Kumar Yadav[1*], Pankaj Singh[1], Sachin Kumar [2]
[*1] Department of Electrical and Electronics Engineering, School of Engineering and Technology, IIMT University Meerut, India
[2] Galgotia Engineering Colleges, Greater Noida, India
[1]talktosujeetyadav@gmail.com and [2]gupta.sachin0708@gmail.com

Abstract

A novel compact radiator UWB MIMO antenna array with the capability to reject WLAN bands is introduced. Two L-strips are loaded in inverted form over a standard rectangular patch antenna to create a protruding radiator for work as radiating element. In this structure, a unique protruding shape antenna with L-shaped slits ground is designed as an antenna array element. Isolation more than -20 dB among the four antenna radiators accomplished by slitting I- shaped slot in the protruding shaped radiator. However, Incorporating L-shaped slot into the ground plane facilitates the desired WLAN band rejection. Diversity performance in relation to mean effective gain (MEG) ratio and envelop correlation coefficient (ECC) are studied. Both simulated and measured results demonstrate that the suggested radiator achieves a broadband performance spanning 2.9 to 16.8 GHz, effectively suppresses the WLAN band, and maintains high isolation among the four radiating elements, confirming the effectiveness of the suggested structure is compatible for ultra-wideband (UWB) applications.

Keywords: Protruding patch antenna MIMO Band-rejection Ultra-wideband (UWB).

1. INTRODUCTION

To ensure optimal performance, MIMO transmitters and receivers are generally equipped with multiple low mutual coupled antenna elements. Conversely, t can cause the antenna housing to become larger, which is the primary limitation of contemporary wireless communication systems. Nonetheless, there will be a noticeable reduction in the Mutual isolation among antenna elements in MIMO systems if multiple antennas are tightly packed together. For a miniaturized MIMO antenna, a strong mutual connection between the antenna's components [1]. In reference [2], A low-profile MIMO antenna array with a compact layout for UWB with two radiating patches. The design incorporates a floating parasitic structure to enhance isolation. To enhance isolation between the two planar radiators, they are positioned orthogonally across a half-sized ground plane by microstrip feeding in [3]. Additionally, [4] achieves compactness, UWB operation, and isolation through the radiator's I-shaped slit being cut and a rectangular stub being attached to the other side. However, [5], depicts a tiny UWB diversity antenna with a meandering path is made by joining a set of smaller L-shaped stubs with an additional inverted L-shaped design parasitic strips, whereby a slot is made in the ground in order to achieve isolation. To accomplish polarization diversity and reduce mutual coupling in MIMO antenna structures, [6] introduced a bent slit is incorporated into each radiating element to realize a notch band at the WLAN. In addition, Koch fractal geometry is employed to enhance isolation between the ports. However, band rejection at the WLAN. The desired band is realized by removing the C-shaped slot from the monopole structure in [7] and [8] Split-ring resonator (SRR) slits were incorporated to achieve band rejection. A couple of L-shaped incisions provided a notched band in reference [9], A T-shaped parasitic element is

Received: August 02, 2025

strategically positioned between radiators to reduce mutual coupling, and an offset fed rhombic slot antenna element is employed to offer a wider impedance spectrum. In reported work [10], presented a UWB MIMO antenna structure that established mutual connection between the two radiators through the placement of two identical heptagonal mono-pole elements on the substrate at a straight angle. Each antenna element contains an etched slit that produces a WLAN band frequency rejection.

Reference [11] states that low mutual coupling is possible when the ground plane and band-rejection are connected to T- and L-shaped stubs capability at the C-band. Different phase- and amplitude-control reflected in Reference [12]. The current project investigates a compact, protrudent-shaped UWB diversity antenna for WLAN networks that has band-rejection capability and the radiating element produced by fusing two inverted L-strips with a Traditional rectangular patch configurations utilized in the proposed architecture.

In addition, a monopole antenna positioned over a planar ground surface to generate monopole-type radiation characteristics. For instance, an eye-shaped monopole antenna has been developed and fabricated in [13], effectively covering the 3–20 GHz frequency range with a VSWR below 1.5. Additionally, conical monopoles are frequently employed in [14]–[17] to produce vertically polarized omnidirectional patterns. This design choice simplifies both the design and fabrication processes while maintaining desirable radiation characteristics. However, [18]–[21] demonstrated the use of triangular feeding structures and a top hat with two shorted posts to achieve a lower-profile or more compact antenna design. On the other hand, to shrink the profile and volume of designed structure, researcher used resistive loading in [22]-[23] and lossy ferrite dielectric material in [24].

A novel compact radiator UWB MIMO antenna array with WLAN band notched is suggested. Two L-strips are loaded in inverted form over a standard rectangular patch antenna to create a protruding radiator for work as radiating element. In this structure, a unique protruding shape antenna with L-shaped slits ground is designed as an antenna array element. Isolation more than -20 dB among the four antenna radiators is realized by slitting I- shaped slot in the protruding shaped radiator. Suggested antenna has a compact size of 26 × 33 mm^2 is excited by and exhibits sharp WLAN band suppression capability. Both simulated and experimental outcomes confirm that the suggested antenna offers a wide operational bandwidth from 2.9 to 16.8 GHz, along with effective WLAN band suppression and high isolation between elements between four radiator elements.

2. MATERIALS AND METHOD

2.1. Geometrical Layout of the Antenna Design

Figure 1 depict the geometry configuration of the presented UWB-MIMO/diversity antenna incorporates analogous radiators sharing two decoupling structures. Protrudent-shaped radiator is used to enhance the electric field current path. Consequently, miniaturize the size of MIMO antenna. The envisioned radiator elements are made with a combination of two L shaped metallic strips and rectangular stub to design a protrudent shaped antenna structure. Pairing of two triangular shaped structures and inverted T shaped structure is employed design the decupling structure. However, a thin type rectangular slots is employed enhanced the isolation between four antenna elements. Finally, the notched band around at 3.45 GHz band (WLAN) is accomplished by cutting two L shaped slots at the ground plane. Four elements were integrated into the ground plane developed using a

International Journal of Applied Mathematics
Volume 38 No. 10s, 2025
ISSN: 1311-1728 (printed version); ISSN: 1314-8060 (on-line version)

1.6 mm thick dielectric sheet with a relative permittivity of 4.4 and a loss tangent of 0.02. A rectangular microstrip feed line (Lf×Wf) is employed to excite the radiator in Table 1.

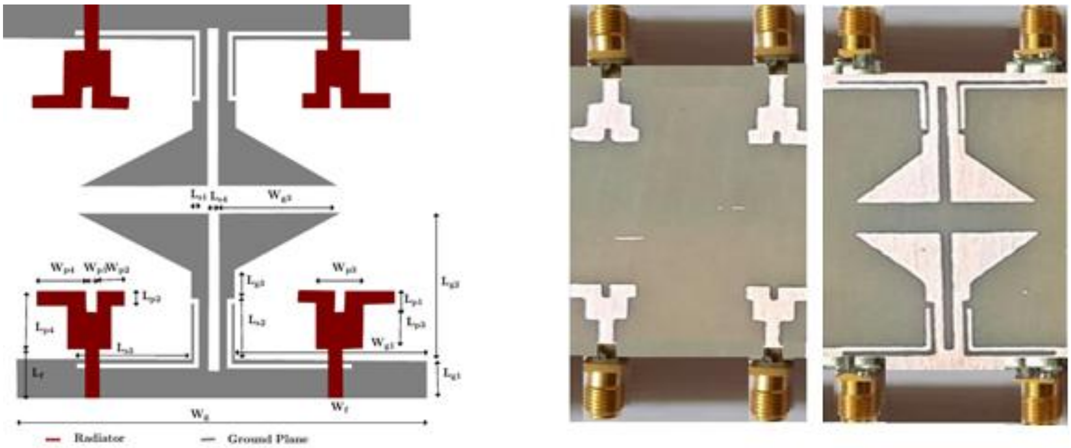

Figure 1. Geometric measurements and fabrication. (a) design of four element antenna. (b) fabrication of radiators and ground plane.

Table 1. The design specifications of the suggested antenna with the dimensions

Specifications	L	Lg1	Lg2	Lg3	Lf
Values (mm)	33	3.23	11.75	2.34	5.5
Specifications	Lp1	Lp2	Lp3	Ls2	Ls3
Values (mm)	1.6	1.45	2.55	4.75	8.45
Specifications	Lp4	Wf	W	Wg1	Wg2
Values (mm)	1.0	1.30	26	10.75	8.85
Specifications	Wp1	Wp2	Wp3	Wp4	
Values (mm)	1.30	3.80	3.85	5.80	

2.2. Evolution of the Radiator

Different layouts employed during the ideation phase for the ideal building were displayed in Figure 2a, in an attempt to achieve broadband performance, patch 1 is placed on one side of the dielectric material and a triangle flag-shaped decoupling structure. The simulated S-parameters for the three-progression radiator is illustrated in Figure 2b.

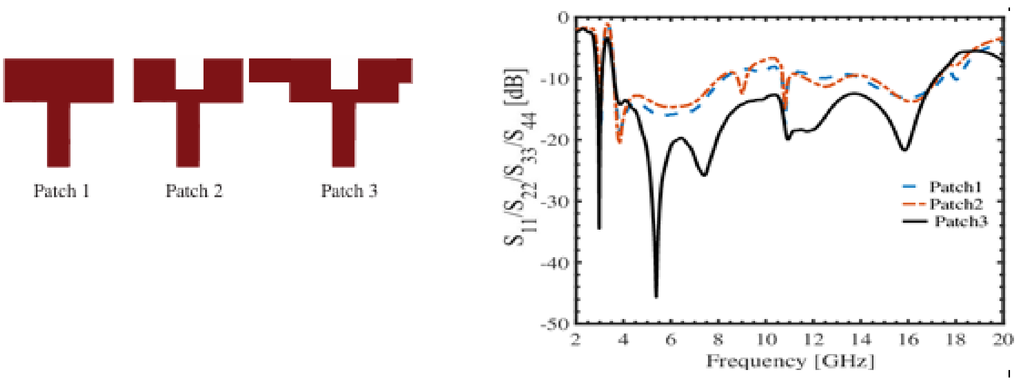

a) (b)

Fig. 2. (a) Progression of proposed radiator (b) simulated S-parameters for different type radiator.

International Journal of Applied Mathematics
Volume 38 No. 10s, 2025
ISSN: 1311-1728 (printed version); ISSN: 1314-8060 (on-line version)

2.2. Evolution of the Radiator

Different layouts employed during the ideation phase for the ideal building were displayed in Figure 2a, in an attempt to achieve broadband performance, patch 1 is placed on one side of the dielectric material and a triangle flag-shaped decoupling structure. The simulated S-parameters for the three-progression radiator is illustrated in Figure 2b.

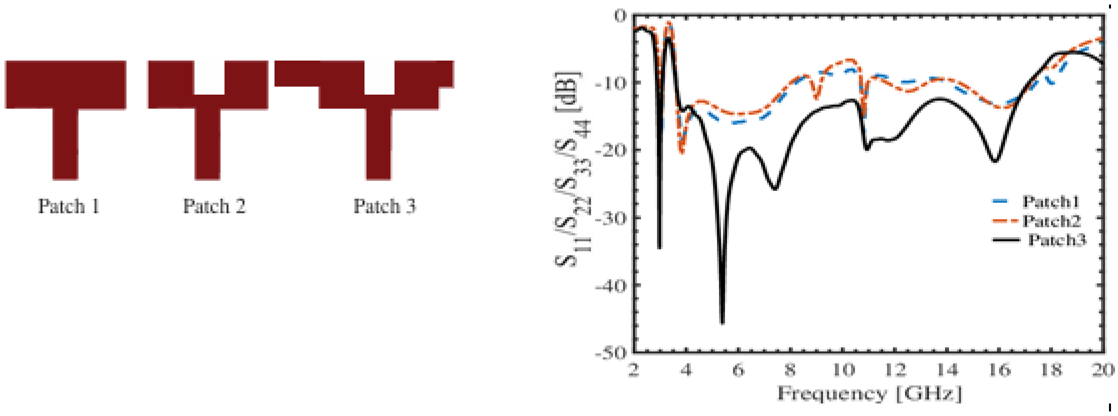

(a) (b)

Fig. 2. (a) Progression of proposed radiator (b) simulated S-parameters for different type radiator.

2.3. Effect of Decoupling Structure

The desired design's performance is significantly impacted by the bottom plane. It not only facilitates improved impedance matching and simultaneously contributes to isolation enhancement through decoupling. Fig. 3 illustrates the stages of evaluation for the decoupling structure growth used in the planned design. The S11 will be the same as S22, S33 and S44 in Fig 4a. Isolation performance better than −20 dB is realized across the full UWB range, as illustrated in Fig. 4b.

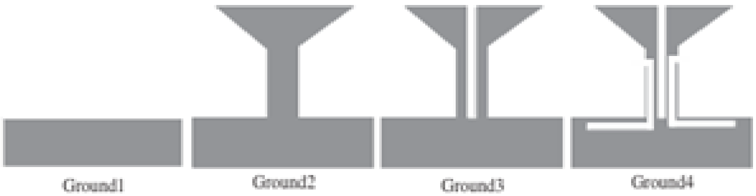

Figure 3. Progression steps for the bottom plane structure

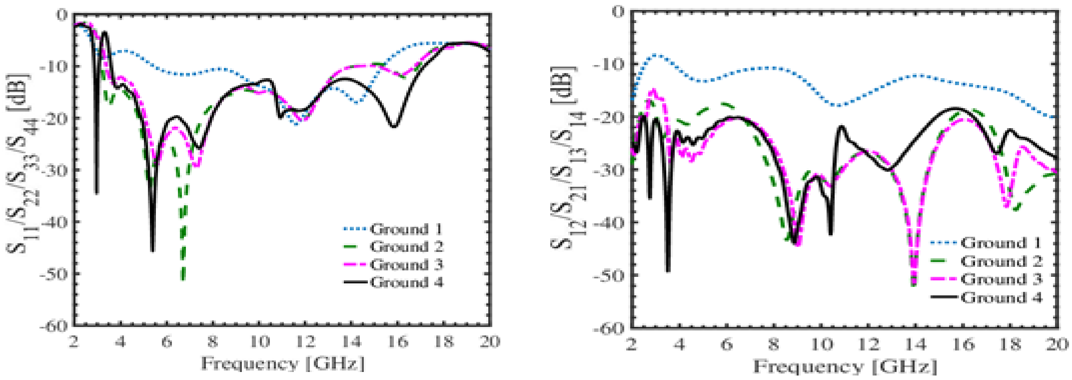

(a) (b)

Figure 4. Simulated S-parameters for different ground shapes (a) $S_{11}/S_{22}/S_{33}/S_{44}$ and (b) $S_{12}/S_{21}/S_{13}/S_{14}$

International Journal of Applied Mathematics
Volume 38 No. 10s, 2025
ISSN: 1311-1728 (printed version); ISSN: 1314-8060 (on-line version)

3. EXPERIMENTAL RESULTS AND DISCUSSION

The planned antenna is manufactured and several characteristics are measured at the antenna measurement laboratory of the Indian Institute of Technology, Roorkee, following optimization. Fig. 2b and Fig. 4b describes the simulated results of the S_{11}. Furthermore, it is observed that the designed antenna's working band from 2.90 to 16.8 GHz, or A wide bandwidth of 13.90 GHz is attained, with mutual coupling among the four radiating elements remaining below −20 dB and effective notch filtering observed at the WLAN band. the diversity antenna's band-rejection performance is demonstrated to be of good quality.

The MIMO performance of the proposed antenna is evaluated using parameters such as envelope correlation coefficient (ECC), mean effective gain (MEG), diversity gain, and total active reflection coefficient (TARC). CC quantifies the level of correlation and mutual isolation between nearby antenna elements and is derived from the S-parameters, as expressed in Equation (1).

$$ECC = \frac{|\sum_{n=1}^{N} S_{i,n}^{*} S_{n,j}|^2}{\prod_{k=i,j}[1-|\sum_{n=1}^{N} S_{i,n}^{*} S_{n,k}|]} \quad (1)$$

Although a detached diversity antenna's ECC value should ideally be zero, a maximum value of less than 0.5 is generally acceptable. Fig. 5a shows the observed and ECC graphs that were simulated for the suggested antenna. It is evident from Figure. 5a that the ECC of the suggested diversity antenna remains under 0.01. The antenna's diversity gain can be computed by:

$$DG = 10\sqrt{1 - ECC^2} \quad (2)$$

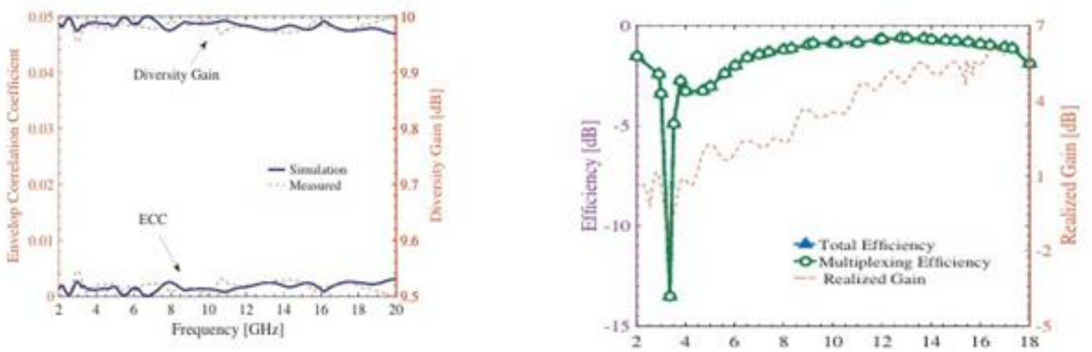

(a) (b)

Figure 5 . (a) Simulation and measured value of the ECC and diversity gain (b) efficiency and realized gain of the designed structure.

The diversity gain using the eq. (2) yield a value of > 9.80 dB, as shown in Figure 5a. and Figure 5b shows the simulated results of the efficiency and realized gain for the diversity antenna's multiplexing efficiency, radiation efficiency, and realized gain. Also, 3D-angular power and multiplexing efficiency (ηMUX), with a wideband performance along with an enhanced signal-to-noise ratio, can be produced as:

$$\eta MUX = \sqrt{(1-|\rho_c|)^2 \eta_1 \eta_2} \quad (3)$$

It is found from Figure 5b that the multiplexing efficiencies and the total efficiency are same. The channel capacity of the system is assessed through the analysis of multiplexing efficiency. Additionally, it is also affect the correlation, total antenna efficiency and efficiency imbalance. The designed antenna attains a gain of 0 to 5.8 dB across the entire

Volume 38 No. 10s, 2025
ISSN: 1311-1728 (printed version); ISSN: 1314-8060 (on-line version)

band and exhibiting a reduction to −2.2 dB within the WLAN rejection region. For a MIMO system, a TARC value remains under 0 dB is optimal. The measured and computed TARC The MEG calculates the proportionate average power of the signals that every radiator provides. The channel characteristics and diversity performance of the antenna will be high if the two radiating component's MEG (|MEG1/MEG2|) ratio is less than ±3 dB. Figure 6a makes it clear that the MEG ratio is staying within the previously stated allowed range throughout the intended antenna's entire operational band16. The effectiveness of multiport antenna systems is affected, as is their entire working bandwidth, when they operate simultaneously, Therefore, relying solely on the S-parameters to define system behavior is insufficient to anticipate actual system behavior. The TARC is an extra parameter that has been added in order to compute the previously indicated effect. TARC is defined as the square root of the total reflected power divided by the total incident power. TARC represents the total diversity antenna system's return loss.

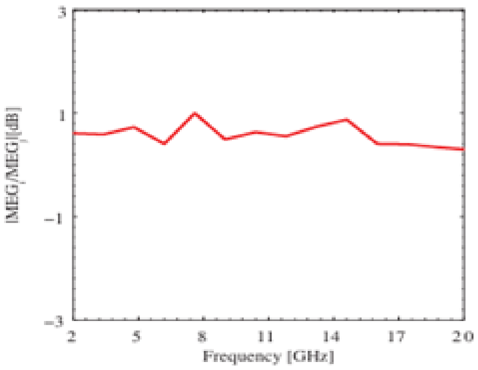

(a)

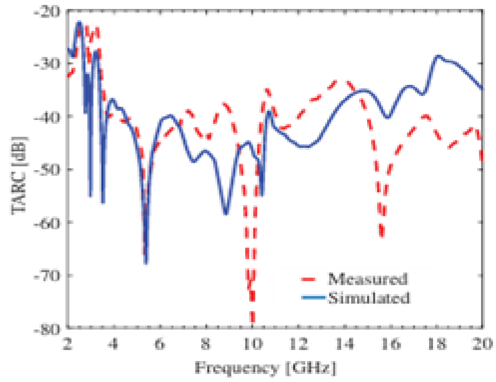

(b)

Figure 6. (a) MEG ratios and (b) TARC with frequency for the designed antenna.

The TARC of a diversity system must be remains under 0 dB over the complete functional bandwidth, the projected antenna exhibits less than −19 dB TARC, as shown in Figure 6b. The radiation pattern graph curves show that the designed antenna's radiation patterns are almost omnidirectional over the whole functional bandwidth as shown in Figure 7.

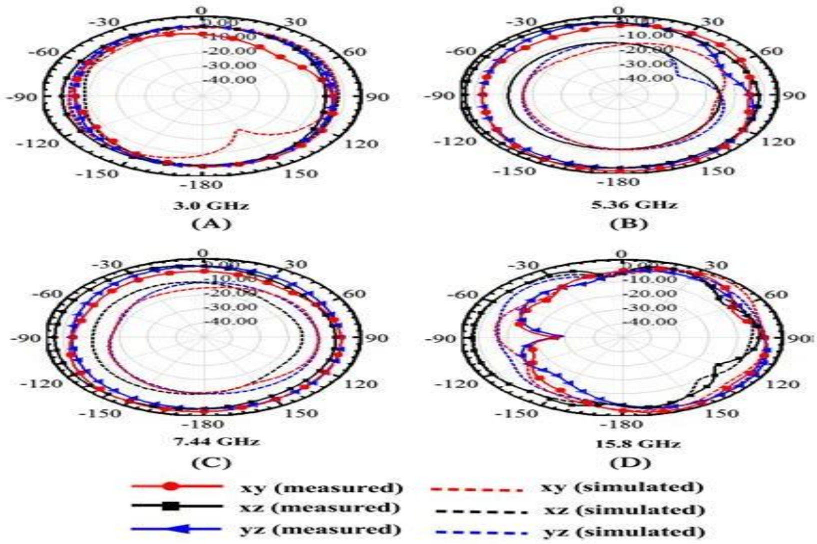

Figure 7. Radiation patterns at (A) 3.1 GHz, (B) 5.30 GHz, (C) 7.55 GHz, and (D) 15.7 GHz.

Received: August 02, 2025

4. CONCLUSION

A novel compact radiator (26 × 33 mm^2) UWB MIMO antenna array with integrated WLAN band rejection is presented. Two L-strips are loaded in inverted form over a standard rectangular patch antenna to create a protruding radiator for work as radiating element. In this structure, a unique protruding shape antenna with L-shaped slits ground is designed as an antenna array element. Isolation more than -20 dB among the four antenna radiators is ensured by slitting I- shaped slot in the protruding shaped radiator. However, the WLAN band rejection capabilities is achieved by inserted L-shaped slits at the bottom plane. Diversity performance in relation to mean effective gain (MEG) ratio and envelop correlation coefficient (ECC) are studied. Simulated and Measured results depict that the designed radiator Maintains wideband characteristics over the range of 2.9 to 16.8 GHz featuring WLAN band rejection and excellent isolation between the four radiator element. These observations affirm the potential of the design for use in UWB band application

FUNDING INFORMATION

Department of Electrical and Electronics Engineering, School of Engineering and Technology, IIMT University Meerut provided funding for the experiments.

AUTHOR CONTRIBUTIONS STATEMENT *(mandatory)* (10 PT)

Sujeet Kumar Yadav performed the simulations, experiment, and drafed the manuscript. Sujeet Kumar Yadav and Pankaj Singh conducted the experiment. Pankaj Singh and Sachin Kumar analyzed the results, proofread the manuscript and supervised the overall work. All authors reviewed the manuscript.

CONFLICT OF INTEREST STATEMENT

The authors declare no Conflict of interests.

DATA AVAILABILITY *(mandatory)* (10 PT)

All data generated or analyzed during this study are included in the published article:

https://doi.org/10.1002/mop.29714

REFERENCES

[1] Vipul Kaushal, Amit Birwal, Kamlesh Patel, “Diversity characteristics of four-element ring slot-based MIMO antenna for sub-6-GHz applications,” Microwave and Optical Technology Letters, vol. 45, pp. 581-593,

[2] Desai, A., T. Upadhyaya, M. Palandoken, and C. Gocen, “Dual band transparent antenna for wireless MIMO system applications,” Microwave and Optical Technology Letters, Vol. 61, 1845-1856, July 2019.

[3] Toktas A, Akdagli A. Compact multiple-input multiple output antenna with low correlation for ultra-wide-band applications. IET Microw Antennas Propag. 2015;9(8):822-829.

[4] Zhang JY, Zhang F, Tian WP, Luo YL. ACS- fed UWB-MIMO antenna with shared radiator. Electron Lett. 2015;51(17):1301 1302.

[5] J.-Y. Deng, L.-X. Guo, and X.-L. Liu, “An ultra wide band MIMO antenna with a high isolation,” IEEE Antenna and Wireless Propagation Letters, vol. 15, pp. 182–185, 2016.

[6] ZhuJ,FengB,PengB,DengL,LiS. A dual notched band and MIMO slot antenna system with Y-shaped defected ground structure for UWB applications. Microw Opt Technol Lett. 2016;58(3):626-630.

ISSN: 1311-1728 (printed version); ISSN: 1314-8060 (on-line version)

[7] Tripathi S, Mohan A, Yadav S. A compact koch fractal UWB MIMO antenna with WLAN band-rejection. IEEE Antennas Wirel Propag Lett. 2015;14:1565-1568.

[8] Gao P, He S, Wei X, Xu Z, Wang N, Zheng Y. Compact printed UWBdiversity slot antenna with 5.5-GHz band-notched character istics. IEEE Antennas Wirel Propag Lett. 2014;13:376-379.

[9] J. Huang, G. Dong, J. Cai, H. Li, and G. Liu, A quad-port dual band MIMO antenna array for 5G smartphone applications, Electronics, vol. 10, no. 5, p. 542, Feb. 2021.

[10] Li R, Mo Z, Sun H, Sun X, Du G. A Low-Profile and High-isolated MIMO Antenna for 5G Mobile Terminal. *Micromachines*. 2020; 11(4):360.

[11] Abdullah M, Kiani SH, Abdulrazak LF, Iqbal A, Bashir MA, Khan S, Kim S. High-Performance Multiple-Input Multiple-Output Antenna System For 5G Mobile Terminals. *Electronics*. 2019; 8(10):1090.

[12] J Zhu, B. Feng, B. Peng, S. Li, and L. Deng, "Compact CPW UWB diversity slot antenna with dual band-notched characteristics," Microwave and Optical Technology Letters, vol. 58, no. 4, pp 989–994, April 2016.

[13] A. Alipour and H. R. Hassani, ''A novel omni- directional UWB monopole antenna,'' IEEE Trans. Antennas Propag., vol. 56, no. 12, pp. 3854–3857, Dec. 2008.

[14] H. Zhai, S. Tjuatja, J. W. Bredow, and M. Lu, ''A quasi-planar conical antenna with broad bandwidth and omnidirectional pattern for ultrawideband radar sensor network applications,'' IEEE Trans. Antennas Propag., vol. 58, no. 11, pp. 3480–3489, Nov. 2010.

[15] W. S. Yeoh and W. S. T. Rowe, ''An UWB conical monopole antenna for multiservice wireless applications". IEEE Antennas wireless Propag. Lett., vol. 14, no. , pp. 1085–1088, 2015

[16] R. Lian, T. Shih, Y. Yin, and N. Behdad, ''A high-isolation, ultrawideband simultaneous transmit and receive antenna with monopole-like radiation characteristics,'' IEEE Trans. Antennas Propag., vol. 66, no. 2, pp. 1002–1007, Feb. 2018.

[17] L. Zhao, Z.-M. Chen, and J. Wang, ''A wideband dual-polarized omnidirectional antenna for 5G/WLAN,'' IEEE Access, vol. 7, pp. 14266–14272, 2019.

[18] S. M. A. M. H. Abadi and N. Behdad, ''An electrically small, vertically polarized ultrawideband antenna with monopole-like radiation characteristics,'' IEEE Antennas Wireless Propag. Lett., vol. 13, pp. 742–745, 2014.

[19] N. Behdad, M. Li, and Y. Yusuf, ''A very low- profile, omnidirectional, ultrawideband antenna,'' IEEE Antennas Wireless Propag. Lett., vol. 12, pp. 280–283, 2013.

[20] K. Ghaemi and N. Behdad, ''A low-profile, vertically polarized ultrawideband antenna with monopole-like radiation characteristics,'' IEEE Trans. Antennas Propag., vol. 63, no. 8, pp. 3699–3705, Aug. 2015.

[21] M. Li and N. Behdad, ''A compact, capacitively fed UWB antenna with monopole-like radiation characteristics,'' IEEE Trans. Antennas Propag., vol. 65, no. 3, pp. 1026–1037, Mar. 2017.

ISSN: 1311-1728 (printed version); ISSN: 1314-8060 (on-line version)

[22] Y. Y. Kyi and J.-Y. Li, ''Analysis of electrically small size conical antennas,'' Prog. Electromagn. Res. Lett., vol. 1, pp. 85–92, 2008.

[23] S. Palud, F. Colombel, M. Himdi, and C. Le Meins, ''Wideband omnidirectional and compact antenna for VHF/UHF band,'' IEEE Antennas Wireless Propag. Lett., vol. 10, pp. 3–6, 2011.

[24] H. Moon, G.-Y. Lee, C.-C. Chen, and J. L. Volakis, ''An extremely lowprofile ferrite- loaded wideband VHF antenna design,'' IEEE Antennas Wireless Propag. Lett., vol. 11, pp. 322–325, 2012.

Received: August 02, 2025